SEGMENT-BASED FOREST VOLUME-BY-TYPE MODELLING USING SMALL FOOTPRINT LIDAR HEIGHT DISTRIBUTIONS

Jan A.N. van Aardt[1], **Randolph H. Wynne**[2]
[1]Department Biosystems (M3-BIORES), Faculty of Bioscience Engineering, Katholieke Universiteit Leuven, Belgium
[2]Department of Forestry, Virginia Polytechnic Institute and State University, USA
E-mail: jan.vanaardt@biw.kuleuven.be

Abstract

This study explored a segment-based approach to coniferous and deciduous forest volume-by-type estimation using small-footprint lidar. The study area is located in the Appomattox Buckingham State Forest (Appomattox County, Virginia, USA) in the Virginia Piedmont physiographic region, and consists of a variety of pine, upland hardwood, and mixed stands. A multiresolution, hierarchical segmentation algorithm was applied to a lidar-derived canopy height model. Lidar multiple return distribution characteristics (mode, mean, range, skewness, etc.) were used to develop volume prediction models and classify coniferous and deciduous segments based on *in situ* mapped basal area (BAF) plots. Volume modelling results were promising with adjusted R^2 values of up to 0.66 for coniferous and 0.56 for deciduous species. Object-oriented classification accuracies were as high as 89% (deciduous-coniferous). Results hint at possible operational implementation, especially when the variability in Virginia Piedmont forests is considered. Such a comprehensive lidar-based inventory approach ultimately could lend itself to large scale, precise, and relatively inexpensive inventories.

Keywords: Multiresolution, Segmentation, Object-oriented, Distribution, Modelling

Introduction

Extensive field methods or aerial photography volume tables long have been regarded as the standard methods of forest inventory (Avery and Burkhart, 1994). These methods frequently are time consuming and expensive, but provide unbiased estimates. Synoptic remote sensing could provide a cheaper option for estimation of forest biophysical parameters over large tracts, while potentially also providing accurate and unbiased estimates. The structural nature of lidar height data makes it especially suitable for gauging forest volume and biomass. Lidar-based forest measurements have been shown to be applicable to general forest inventory and canopy structure modelling (Lefsky *et al.,* 2002; Næsset, 2002; Popescu *et al.*, 2004) and have been implemented to gauge forest fuel loads (Riaño *et al.*, 2003; Seielstad and Queen, 2003) and derive digital elevation models (Popescu *et al.*, 2002; Hodgson *et al.*, 2003). Lefsky *et al.* (2002) have proven that lidar sensors can provide accurate and non-asymptotic estimates of various forest indices, e.g., LAI and aboveground biomass. A lidar-based approach to forest inventory furthermore could negate the need for ground-based, small scale measurements of tree heights and/or canopy parameters.

Although large footprint lidar sensors have been used extensively for forest volume and biomass estimation (Lefsky *et al.,* 1999; Means *et al.,* 1999), the spatially discontinuous nature of large footprint lidar sensors limits their applicability at local scales. Small footprint lidar sensors are more amenable to volume and biomass estimation on small tracts of forest and have been used as early as the mid-1980's for forest volume estimation (Maclean and Krabill, 1986; Nelson *et al.,* 1988). Lidar studies have included both plot- and stand-based approaches (Nilsson, 1996; Popescu *et al.*, 2004), while lidar height distributional approaches have come to the fore more recently (Means *et al.*, 2000; Næsset, 2002). These authors exploited the relationships between distributional height metrics, e.g., mean, range, skewness, and percentiles, and forest biophysical parameters. This approach lends itself to segment- or stand-level application and approximates a waveform-type return found in the case of large footprint lidar sensors. These pseudo-waveforms are useful for characterization of vertical forest structure, a feature which is potentially valuable for large scale, stand-level volume- and biomass estimation (Magnussen and Boudewyn, 1998; Means *et al.*, 2000; Drake *et al.*, 2002; Næsset, 2002).

Means *et al.* (2000) implemented a lidar distributional approach to estimate height and basal area for Douglas-fir stands, ranging from shrub-like (18 m^3/ha) to old-growth (1313 – 2051 m^3/ha) stands. Lidar returns were extracted from 10 x 10 m grid cells within larger 50 x 50 m measured plots. Distributional parameters, e.g., canopy cover percentiles, maximum height, elevation, average mean height, and average of the maximum heights were calculated for grid cells. Stepwise regression analysis was used to determine the relationships between ground data and lidar measurements, with dependent variables height, basal area, and volume. R^2 values of 0.93 (RMSE = 3.4 m), 0.95, and 0.97 (no RMSE for latter two values) were obtained for height, basal area, and volume, respectively. R^2 values for plots excluding old-growth plots were 0.98 (RMSE = 1.7 m), 0.94 (RMSE = 5.4 m^2/ha), and 0.95 (RMSE = 73 m^3/ha), for height, basal area, and volume, respectively. Various percentile variables, e.g., the 90^{th} height percentile and 20^{th} coverage percentile, were shown to be significant predictor variables. Næsset (2002) predicted volume and crown parameters for Norway spruce (*Picea abies*) and Scots pine (*Pinus sylvestris*) stands in Norway, using a stratum-specific (young forests; old-growth, on poor and good sites) approach. Observed volume values ranged between 41 m^3/ha and 639.8 m^3/ha. Lidar first- and last pulse distribution based regression equations were used to model volume and crown parameters. Various quantiles, maximum- and mean values, canopy density measures, and coefficients of variation were used as independent variables. R^2 values for 61 reference stands were 0.87 (dominant height) and 0.91 (volume). Standard deviations ranged between 0.7 – 1.33 m (dominant height) and 18.3 – 31.9 m^3/ha (volume).

The extension of distributional grid-cell approaches to object- and stand-level applications was deemed the next logical step. According to Burrough and McDonnel (1998), an object (segment) refers to a spatial entity that is homogenous in terms of a selected property, as opposed to the traditional, continuous field approach found in spatial analysis. Segments therefore can be treated as entities or objects, since each segment is homogenous in terms of a defined variable. Douglas *et al.* (2003) have shown that such an application requires that distinct forest cover and structural types have different, unique lidar canopy densities or distributions. Segment-level estimate errors also can be minimized (Makela and Pekkarinen, 2001; Pekkarinen, 2002). Segment-based modelling furthermore is amenable to stand-level scaling, since segments can match existing structural boundaries in forests, but this based on the assumption that segments are hierarchical and topologically sound.

The basic precept of this study was that extraction of lidar distributions on a grid-cell basis, used to model volume and biomass (Means *et al.*, 2000; Næsset, 2002) and classify forests, could be extended to estimation/classification at the segment level. The specific objectives of this study therefore were (i) to determine whether volume and aboveground biomass estimation and (ii) mapping of 2-class (deciduous-coniferous) and 3-class (deciduous-coniferous-mixed) segments in the Virginia Piedmont successfully can be performed using object-oriented analysis of lidar distributions.

Materials and Methods

Study Area and Data

The 946 ha study area is located in Appomattox Buckingham State Forest (Appomattox County) in the Piedmont physiographic province of Virginia, southeastern U.S.A at 78°41' W, 37°25' N (Figure 1). The mean elevation of the study area is 185 m (606 ft.), with minimum and maximum elevations of 133 m (436 ft.) and 225 m (738 ft.), respectively. Local topography can best be described as gentle rolling slopes and flat terrain. Vegetation is composed of various coniferous (*Pinus taeda, P. virginiana, P. echinata*, and *P. strobus*), deciduous (*Quercus coccinea, Q. alba,* and *Liriodendron tulipifera*), and mixed forests.

Lidar data (2002) were acquired by Spectrum Mapping using the DATIS II (small-footprint, high-density, multiple return) system (Table 1). Field data consisted of 256 mapped basal area plots (BAF; basal area factor 10) on a 16 columns by 16 rows, 201.17 m (10 chains) grid spacing. Field data were collected during the summer, fall, and winter months (May – December) of 2003. Differentially corrected plot location, plot basal area, and diameter at breast height (dbh), height, and species were determined for all plots and tallied trees. A total of 37 plots were located on private land or had basal area values of zero (no type differentiation possible), which left 219 BAF plots for use in the statistical analysis.

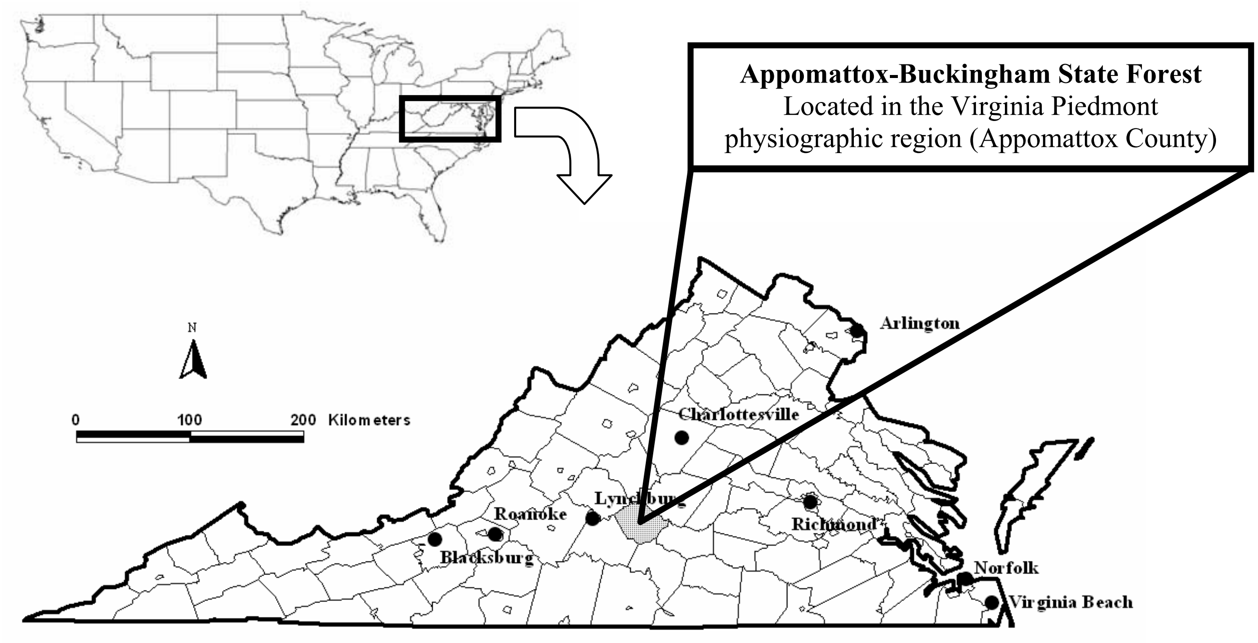

Figure 1. Study Area: Appomattox Buckingham State Forest

Table 1. DATIS II lidar data set characteristics

Characteristic	Specifications
Laser altitude	2,000 m (6,562 ft.) above ground level
Laser scan field-of-view	75° maximum
Swath width and centreline spacing	800 m (2,625 ft.) and 400 m (1,312 ft.)
Scan rate	25 Hz
Laser pulse rate	35 kHz
Scan angle	± 13.5°
Returns	≤ 5
Resolvable distance between returns	0.75 m
Footprint	0.46 m (1.51 ft.)
Spacing across / along track	1 m (3.3 ft.) / 2 m (6.6 ft.)
Accuracy (X,Y,Z)	X,Y: 0.5 m; Z: 0.15 m (X,Y: < 1.6 ft.; Z: < 0.49 ft.)
Post-processed GPS accuracy	< 0.05 m
Wavelength	1,064 nm

Basal area percentages were used to assign plots to 2- and 3-class forest type schemes. A strict majority rule was used to assign "Deciduous" (140 plots) or "Coniferous" (79 plots) types, while a "Mixed" class was used in the 3-class type designation for plots that had less than 90% basal area contribution for either of the two pure types. The 90% cut-off was due to the fact that the 3-class analysis consisted of 112 deciduous, 56 coniferous, and 51 mixed plots, which allowed for volume and biomass model development based on adequate plot samples (> 30). For instance, only 25 (11.4%) of the plots were mixed when a 75% cut-off was used, resulting in a class that was too small for viable statistical analysis.

BAF plots were expanded to a per-hectare basis for each segment. This was done using standard BAF expansion equations (Avery and Burkhart, 1994). Single-tree volume and biomass equations (Saucier and Clark, 1985; Clark *et al.*, 1986; Schroeder *et al.*, 1997; Sharma and Oderwald, 2001) were used, with specific volume and biomass equations for loblolly and other southern pines, as well as for hardwoods. Plots were assigned to the segment in which they were located through post-stratification of selected segmentation results. BAF plot values were averaged in cases where larger segments contained more than one field plot. Descriptive statistics for all basal area plots are given in Table 2.

Table 2. General descriptive information for deciduous, coniferous, and mixed plots

Class	Type	Parameter	Minimum	Maximum	Average	σ
2-class	Deciduous plots (140)	Volume/ha (m^3/ha)	6.94	350.65	157.64	84.14
		Biomass/ha (Mg/ha)	11.11	269.01	113.60	58.60
		Basal area/ha (m^2/ha)	2.30	34.44	16.32	7.84
	Coniferous plots (79)	Volume/ha (m^3/ha)	8.32	350.93	114.49	75.44
		Biomass/ha (Mg/ha)	4.67	155.56	41.47	26.64
		Basal area/ha (m^2/ha)	2.30	36.73	14.24	7.91
3-class	Deciduous plots (112)	Volume/ha (m^3/ha)	6.94	350.65	156.16	89.32
		Biomass/ha (Mg/ha)	11.11	269.01	117.31	62.53
		Basal area/ha (m^2/ha)	2.30	34.44	15.97	8.21
	Coniferous plots (56)	Volume/ha (m^3/ha)	8.32	278.99	100.45	66.42
		Biomass/ha (Mg/ha)	4.67	81.65	33.66	19.95
		Basal area/ha (m^2/ha)	2.30	36.73	13.61	8.11
	Mixed plots (51)	Volume/ha (m^3/ha)	31.68	350.93	156.85	72.60
		Biomass/ha (Mg/ha)	20.06	175.75	81.49	38.93
		Basal area/ha (m^2/ha)	4.59	36.73	16.84	6.68

Lidar Data Processing

A canopy height model (CHM) was derived for subsequent segmentation efforts. First and last, bare-soil lidar returns, as supplied by the data provider, were interpolated to a 1 m spatial resolution grid using regular Kriging (Popescu *et al.,* 2002). Interpolation was performed using Surfer 7.0 software (Golden Software, Inc.). First return data were assigned to top-most canopy heights, while last, vegetation–removed returns were attributed to ground hits. The differenced first- and bare-soil return surface (CHM) was used as input to the eCognition segmentation algorithm. This allowed for extraction of forest segments based on height homogeneity and distinct stand breaks, e.g., roads and slope breaks.

Raw lidar data had to be processed on a per-return basis so that information related to the return hierarchy was retained for use in the distributional approach. Ground hits, regarded as an important component of overall lidar distributional patterns, were removed for each unprocessed lidar return file using Terrascan V. 003.002 (Terrasolid, Inc.) and MicroStation V. 08.00.04.01 (Bentley Systems, Inc.) software.

Non-ground hits, designated as vegetation hits, were normalized for varying terrain elevations (Means *et al.*, 2000) by calculating the difference between the vegetation hit and the bilinear interpolated height of the four corner cells of the DEM cell directly beneath each hit.

Segmentation of the Study Area

The multiresolution, hierarchical eCognition V. 3 algorithm (Definiens) was used to segment the lidar-derived CHM of the study area. The goal was to derive unique structural segments based on lidar data, a structural data type. The eCognition algorithm required Color:Shape and Smoothness:Compactness ratios as input parameters. The Color:Shape ratio was set at 0.8:0.2, based on the recommendation of the developers (Baatz and Schäpe, 2000; eCognition, 2003) and visual inspection of results when using alternative parameter inputs. Segment smoothness was considered more important than shape in a forestry context, since smooth, boundary-following segments are preferable to compact, blocky segments. The Smoothness:Compactness weight combination therefore also was set at 0.8:0.2. eCognition was the chosen segmentation algorithm because of its hierarchical nature, correspondence to input data, and since results from this algorithm have been validated in the natural resources context (Kayitakire *et al.*, 2002; Nugroho *et al.*, 2002; Kressler *et al.*, 2003). One could, however, argue that the segmentation method is subordinate to the utility that resultant objects have to analyses.

Segmentation results were chosen for subsequent analysis based on average segment size. These ranged from average BAF plot area, with radii defined by average tallied tree distance from field-collected BAF plot centres, plus one and two standard deviations, to the segment sizes where within-segment variance was smaller than between-segment variance of the CHM heights. This procedure ensured that segments with limited within-segment variability were selected for analysis. Ten average segment sizes, ranging from 0.035 ha/segment to 3.942 ha/segment, therefore were chosen for subsequent volume and biomass model development and forest type classification. The segmentation result that approximated the average Appomattox stand area, as well as the actual stands, also was included in the analysis. Selection of the stand-corresponding segment size made comparison of segmentation-based modelling and stand-based modelling possible. Vegetation and ground lidar data sets were extracted on a per-segment basis for all segmentation results using ARCGIS V. 8.3 software (ESRI). Resultant data sets were exported to SAS V. 8.02 software (Level 02M0; SAS, Inc.) for subsequent regression analysis.

Regression and Classification Analysis

Distributional parameters were derived only for first and second return vegetation data sets, since multiple segments had missing parameter values for the third through fifth returns. Distributional parameters included the mean, coefficient of variation, kurtosis, maximum, minimum, mode, range, standard error of the mean, skewness, standard deviation, number of observations, height percentile points at 10% intervals of height values, and canopy cover percentiles. Canopy cover percentiles were based on the proportion of first returns smaller than a given percentage of maximum height, e.g., the 10% canopy cover percentile included all first returns lower than 10% of the maximum height for that segment. The ratio of the number of vegetation or ground hits and the total number of lidar hits per segment also was calculated. This was done for second, and third through fifth group vegetation hits, as well as first, second, and third through fifth group ground hits. The vegetation ratio for each segment was calculated as the ratio of the number of vegetation hits per segment and the total hits for that segment. Means *et al.* (2000) has shown that these distribution metrics are useful descriptors of tree volume for 10x10 m grid cells in Douglas-fir, western Oregon stands, while Næsset (2002) used the same approach for 200 m^2 sample plots in Norway spruce and Scots pine stands in southeast Norway. Lidar intensity distributional parameter values for the first and second returns included the intensity mean, median, coefficient of variation, maximum, minimum, range, standard error of the mean, and standard deviation.

Linear regression analysis, with segment volume and biomass as dependent variables, and discriminant classification were performed as follows:

- Variable reduction was done by using a forward selection process with α-values set between 0.075 and 0.350 as significance levels for remaining in the model. The goal was to reduce independent variables from 75 initial variables to fewer than 10 variables in all cases.
- Validation of selected variables was performed using Pearson's correlation coefficients between independent and dependent variables. All variables with correlations of 0.8 or lower were retained, while only the variable with the highest correlation to the dependent variable (volume/biomass/type) was retained in cases where independent variable correlations were higher than 0.8. A value of 0.8 was chosen based on data characteristics, with the knowledge that all lidar-derived variables are height-related, resulting in inherently high correlations. Statistically invalid models (overfitting) were thereby avoided in the final regression step, namely linear regression using Mallow's Cp and adjusted R^2 as selection criteria.
- Mallow's Cp selection takes all combinations of independent variables into account, while calculating a value related to the mean square error of a fitted value for all models (Draper and Smith, 1981; Montgomery *et al.*, 2001). RMSE (where applicable), model simplicity, and model validity also were considered.
- A discriminant classification approach, similar to the one used by van Aardt and Wynne (2001), was applied to the lidar distributional parameters for forest type classification. It has been shown that discriminant approaches, as opposed to non-parametric classifiers, are better suited to the classification of images where training data exhibit distinct overlap in the feature space (Cortijo and De la Blanca, 1999).
- General classification statistics (cross-validation), including overall accuracy, user's and producer's accuracies, and Kappa-statistics (Congalton and Green, 1999), were calculated for all segment sizes. A normalized z-test statistic, derived from the proportion of correctly classified samples ($\alpha = 0.05$; H_0 = no difference between classification accuracies for different segment sizes; H_0 rejected if $z > 1.96$) (Foody, 2004), was used to compare classification outcomes for different average segment sizes. Samples were considered independent, given the variable sample numbers for different segment sizes. The standardized normal test statistic for cases with independent test samples is given by:

$$z = \frac{\frac{x_1}{n_1} - \frac{x_2}{n_2}}{\sqrt{p(1-p)\left(\frac{1}{n_1} + \frac{1}{n_2}\right)}} \qquad [1]$$

where x1, x2 = correctly allocated number in two independent samples of size n_1 and n_2, respectively; p = $(x_1 + x_2)/(n_1 + n_2)$ Foody, 2004)

- Significance tests were performed for both 2- and 3-class classification schemes and were iteratively repeated for the highest and lowest accuracies in ascending order if the two extreme accuracies were significantly different from each other. This was done until no significant differences between the highest accuracy and the other accuracies were found. It should be noted that accuracies could be found significantly different by chance alone, given the number of possible comparisons among twelve segmentation treatments. These tests were based on a standard T-test (α = 0.05) with paired samples (average segment size) for differences between classification accuracy means.

Regression analyses and classification were performed for segmentation results of 0.035 ha/segment, 0.091 ha/segment, 0.141 ha/segment, 0.318 ha/segment, 0.642 ha/segment, 0.964 ha/segment, 1.263 ha/segment, 1.885 ha/segment, 2.53 ha/segment, 3.942 ha/segment, 5.632 ha/segment, and the Appomattox Forest stands (5.666 ha/segment). Models were fitted to “Deciduous” and “Coniferous” groups, as well as for all segments combined. Deciduous segments ranged between 61 and 140 segments and coniferous segments between 34 and 79 segments, depending on the average segment size and number of BAF plots that were averaged for larger segment sizes. Analyses were performed on “Deciduous” (43 - 112 segments), “Coniferous” (22 - 56 segments), and “Mixed” (30 - 51 segments) classes in the case of the 3-class forest scheme. Analyses were limited to segments with non-missing values for distributional parameters. The only case with missing distributional parameter values occurred at 0.035 ha/segment (27,050 segments) for the 2-class (16/140 deciduous and 9/79 coniferous missing segments) and 3-class (14/112 deciduous and 1/51 mixed missing segments) forest definitions.

Results and Discussion

The various variable reduction methods were successful in reducing independent variables from the original 75 variables to fewer than 10 in each case. There were no distinct trends in selected variables, with vegetation hits from the 1st and 2nd returns, intensity variables, percentiles, canopy cover percentiles, and ratio variables all well represented across forest types and segmentation treatments. However, intensity mean, maximum, and range variables of both first and second return vegetation hits were especially well represented. This corroborated findings by Means *et al.* (1999) and Brandtberg *et al.* (2003) and indicated that intensity values are of significance in the modelling of forest biophysical parameters. The representation of intensity values (near-infrared: 1,064 nm) as part of variables selected for classification was especially evident, with the median intensity of first return vegetation heights present in all data sets. Other studies have found near-infrared wavelengths to be highly discriminant among vegetation types, especially between deciduous and coniferous species (Martin et al., 1998; van Aardt and Wynne, 2001). The broad range of selected variables, in general, build a strong case for the use of multiple return lidar data and associated intensity-per-return when modelling forest biophysical parameters. This might be especially critical in areas that contain forests with high variability in site, growth, and composition. Second returns, which contribute to defining height levels other than the topmost canopy and describe aspects of forest vertical structure besides canopy height, also were prevalent.

Figure 2 indicates that lidar height distributions were representative of BAF plot measurements. Low-volume segments exhibited either fewer hits at taller tree heights, or generally shorter trees than segments with higher volume-per-hectare measurements, while distributions for lower volume-per-hectare segments also were skewed to the right, and *vice versa*. Distributions such as these served to illustrate why variables such as percentile, skewness, canopy cover, and kurtosis variables were selected. Figure 3, on the other hand, shows an example of deciduous and coniferous segments with similar volume-per-hectare values across increasing average segment sizes. Distributions visually remained similar in shape as average segment size increased. The increase of upper- and lower tail values in the case of deciduous segments was attributed to trees of above-average height and undergrowth, respectively, commonly found in an uneven-aged stand.

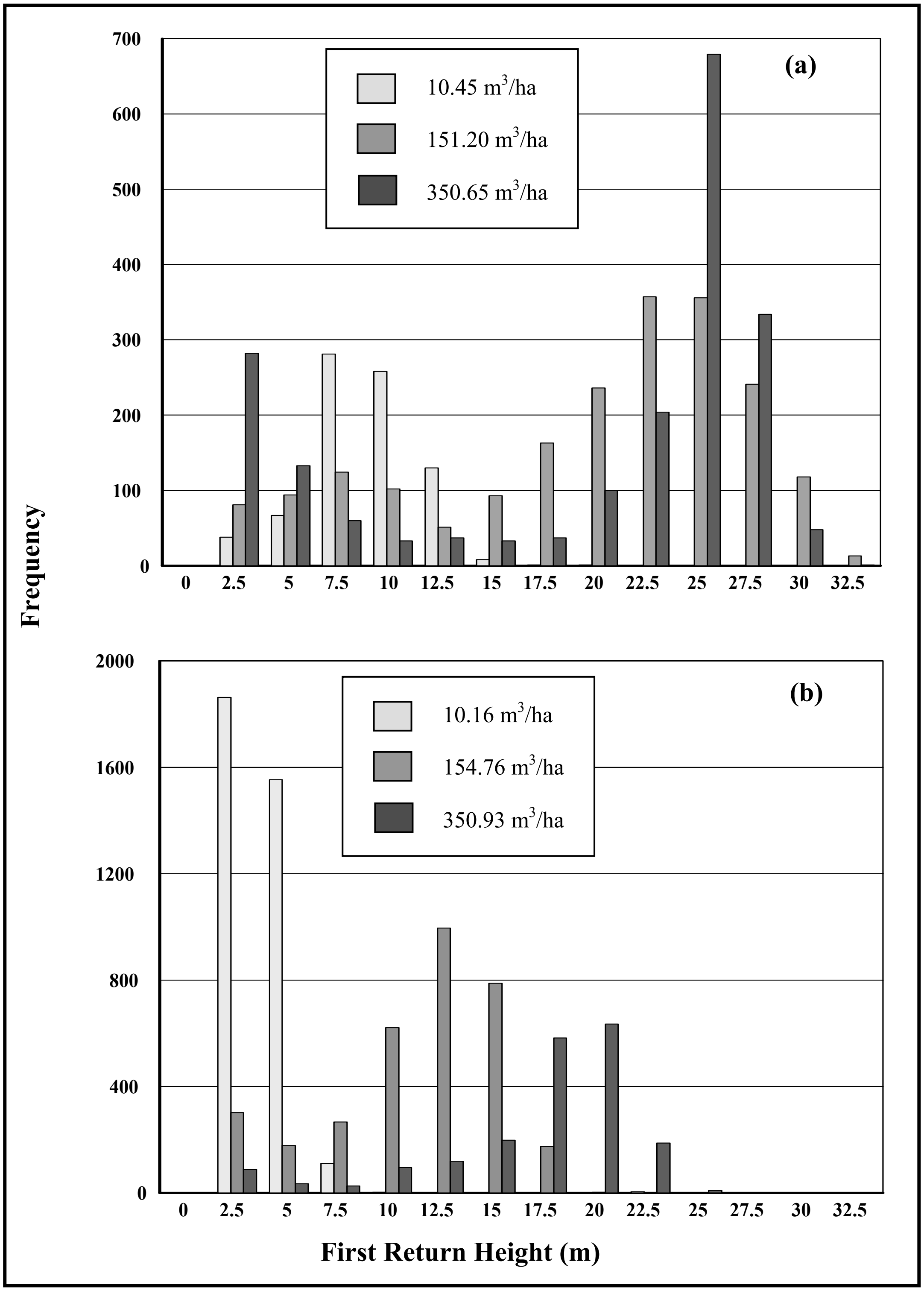

Figure 2. (a) Deciduous and (b) coniferous per-object (0.035 ha/object) histogram plots for lidar first return vegetation hits across a range of field-measured volume-per-hectare

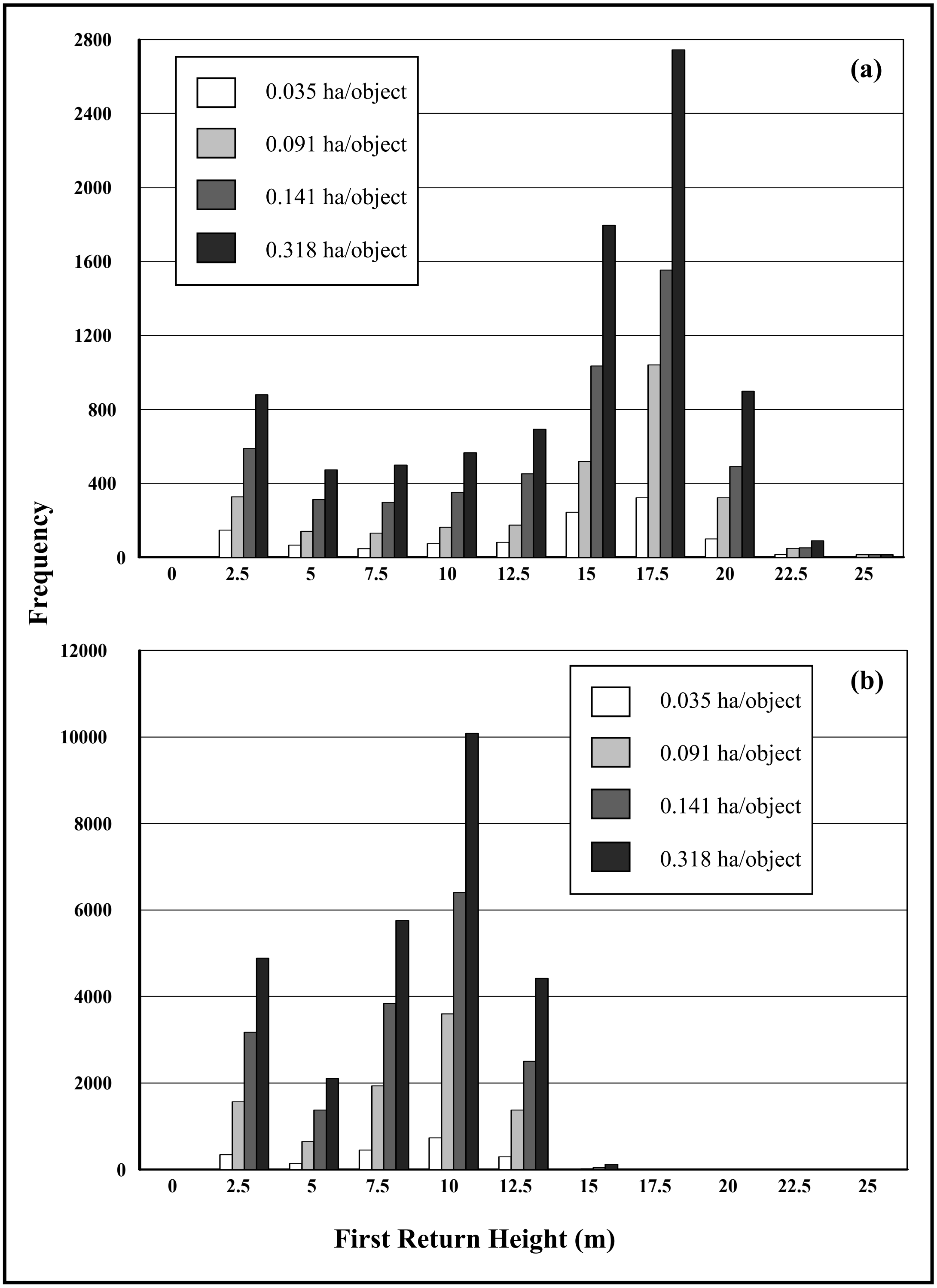

Figure 3. (a) Deciduous and (b) coniferous first return, vegetation height distributions for variable size objects with 153.02 m^3/ha and 159.50 m^3/ha volume, respectively

Table 3 shows the best performing models (adjusted R^2) and associated descriptive statistics for 2- and 3-class forest schemes and the Appomattox stands. Residual behaviour for the best performing 2-class volume and biomass models, 5.632 ha/segment and 0.091 ha/segment, respectively, are shown in Figures 4 and 5. The majority of models could be limited to 5 or fewer independent variables, except for coniferous volume and biomass models, which was attributed to increased variation present in the case of coniferous segments. Highly variable stands are common in the Virginia Piedmont, since pure forest stands in public ownership are relatively limited. A deciduous-coniferous stand likely added more variability to the coniferous group, whereas mixed deciduous stands have similar characteristics.

Table 3. Volume and biomass models with the highest adjusted R^2 values for volume and biomass modelling for 2- and 3-class schemes

Model			Segment adjusted R^2	Stand adjusted R^2	Segment RMSE (m^3/ha or Mg/ha)	Stand RMSE (m^3/ha or Mg/ha)	Segment size (ha)
2-class Volume	D	262.37385 + 19.92957 P_Veg2_70 + 208.14833 ZeroNgrnd3_5ratio -387.67008 Canopy80P	0.59	0.44	51.15	63.56	5.632
	C	458.52340 -4.18276 ModeVeg1 + 15.43186 P_Veg1_40 -5.59238 RangeVeg2 -0.36692 StdInt2	0.66	0.48	38.03	55.61	5.632
	A	309.84855 + 0.29731 CVVeg1 + 13.66277 MinVeg1 + 11.12989 P_Veg1_50 - 0.14246 MedianInt1 -432.13149 MinVeg2 + 55.39894 Canopy30P	0.59	0.42	53.75	62.36	0.091
2-class Biomass	D	271644 + 13993 P_Veg2_75 -286090 ZeroNVeg2ratio -75577 Canopy70P	0.58	0.43	37.41	45.84	5.632
	C	185653 + 2262.86568 P_Veg1_20 - 29.74409 MedianInt1 + 3533.08872 P_Veg2_40 -91682 Vegratio -20694 Canopy70P	0.59	0.40	17.15	19.45	0.091
	A	343583 -1370.95705 CVInt1 + 316.85290 CVVeg2 + 15082 P_Veg2_75 -132911 ZeroNVeg3_5ratio -314776 Canopy80P	0.66	0.46	33.14	41.18	5.632
3-class Volume	D	-31.77814 + 19.67658 P_Veg2_70	0.62	0.46	55.98	68.16	5.632
	C	303.72815 + 15.71060 P_Veg1_30 - 1.78646 StdMeanInt2 -0.59669 StdInt2 + 0.06230 MedianInt2 + 737.63803 ZeroNgrnd1ratio + 146.83730 Canopy70P	0.67	0.73	38.24	40.08	0.642
	M	255.71328 -3.17225 ModeVeg1 + 1.54155 MinInt1 -5.84654 StdMeanInt2 -444.06932 ZeroNgrnd1ratio -111.50951 Canopy10P - 145.92581 Canopy50P -413.21393 Canopy80P	0.74	0.57	28.02	46.68	5.632
3-class Biomass	D	-134083 + 16205 P_Veg2_75 + 2460.48834 StdMeanInt2 + 159205 ZeroNgrnd3_5ratio	0.62	0.46	39.48	48.61	5.632
	C	-84498 + 6498.76606 P_Veg1_25 + 44.56384 MedianInt1 -81.96051 StdInt2 + 78560 ZeroNgrnd3_5ratio	0.63	0.70	12.06	12.56	3.942
	M	1493940 -601912 MinVeg1 + 4984.27818 P_Veg1_10 -370.80540 RangeInt1 + 84546 ZeroNVeg3_5ratio -612016 Canopy80P	0.79	0.68	16.32	20.29	5.632

Veg = Vegetation lidar hit; Grnd = Ground lidar hit; Int = Intensity associated with lidar hit; Veg1, 2, or 3_5 = 1^{st}, 2^{nd}, or grouped 3^{rd} through 5^{th} returns; P_..._10-90 = Percentiles; CV = Coefficient of variation; StdMean = Standard error of the mean; Std = Standard deviation; Canopy10-90 = Canopy cover percentiles; N..ratio = Vegetation or ground hits as a ratio of return totals; Vegratio = Vegetation hits as a ratio of total hits

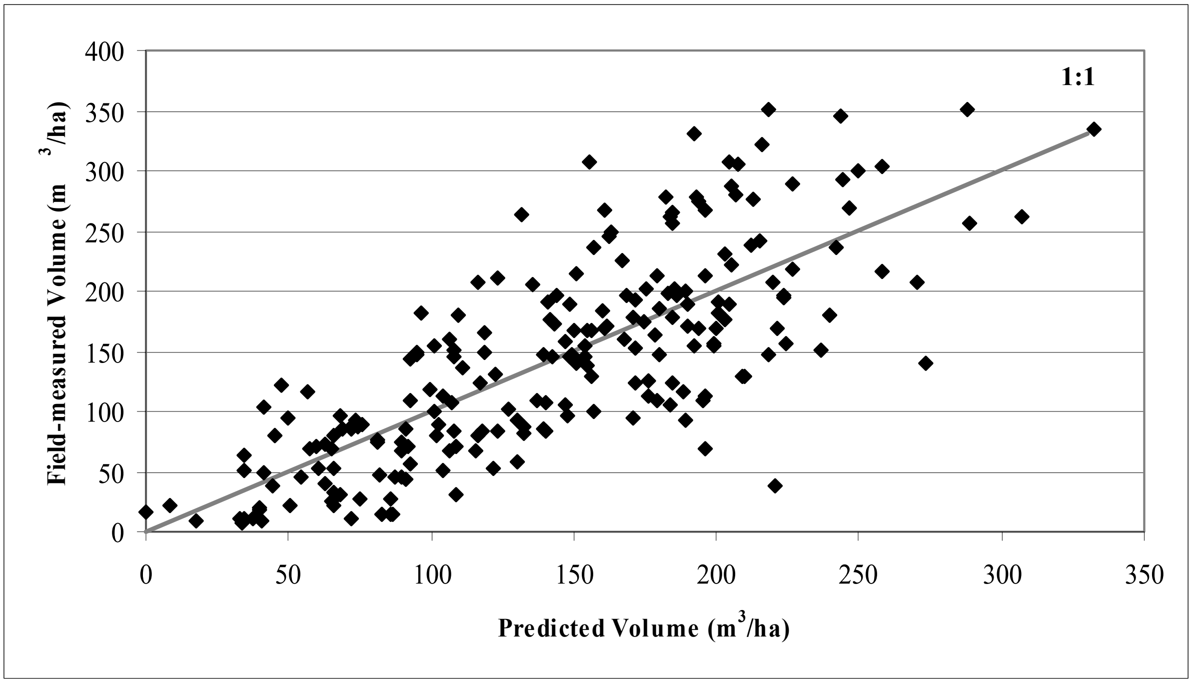

Figure 4. Two-class volume model (0.091 ha/segment): Field-measured vs. predicted volume/ha values for all plots combined (adjusted R^2 = 0.59)

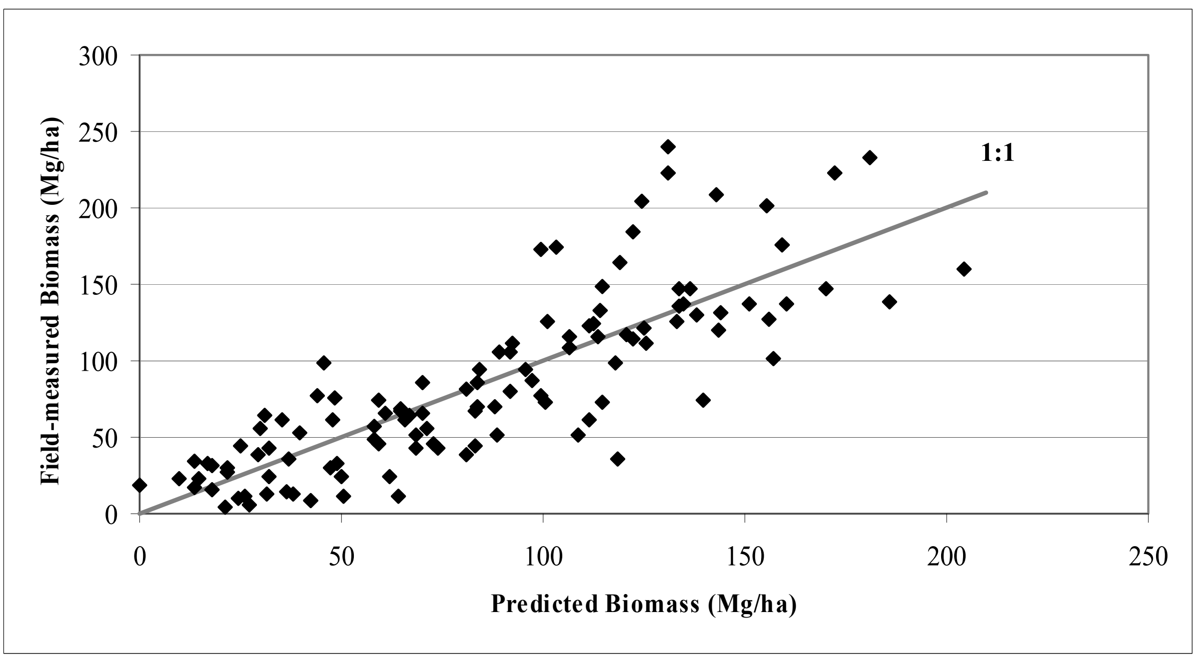

Figure 5. Two-class biomass model (5.632 ha/segment): Field-measured vs. predicted biomass/ha values and residuals for all plots combined (adjusted R^2 = 0.66)

Adjusted R^2 values for coniferous species volume were lower than those found in two comparable studies by Means *et al.* (2000; adjusted R^2) and Næsset (2002; R^2), both of which used a grid-cell based lidar distribution approach to volume modelling. The range of forest volume and growth-types, low single species variability, averaging effect of plot-based measurements, and fixed plot measurements that directly corresponded with lidar plot boundaries could have contributed to higher R^2 values in these two studies. RMSE values, on the other hand, were comparable to those found by Means *et al.* (2000; 73 m^3/ha, old-growth plots excluded) and Næsset (2002; 18.3 – 31.9 m^3/ha). This indicated that a segment-based approach has potential for extension to operational application, since it could be argued that RMSE values (estimate and precision) operationally are more important than R^2 values.

Coniferous adjusted R^2 values for volume in this study ranged from 0.46 (2-class; 1.885 ha/segment) to as high as 0.67 (3-class; 0.642 ha/segment. Lower adjusted R^2 values were attributed to a narrower range in volume and biomass-per-hectare values for this study (6.94 – 350 m^3/ha; 4.67 – 269.01 Mg/ha). This was due to more intrinsic variability found in this narrower range, while an increased observed range with lower variability likely will result in better model fit statistics. Plot sampling technique also was a potential source of variability. Unlike the complete grid-cell inventory by Means *et al.* (2000), not every tree within a segment was measured in this approach. Although BAF plot measurement is an established forestry inventory technique, it does not account for all trees on a given plot. Each segment was assumed to be represented by its enclosed BAF plot. This assumption also could have impacted the results.

Adjusted R^2 values for deciduous types were significantly higher than those calculated for a plot-level lidar study in the same area Popescu *et al.* (2004). Values of 0.59 (2-class; 5.632 ha/segment) and 0.62 (3-class; 5.632 ha/segment) compared well to an unadjusted R^2 of 0.36 found by Popescu *et al.* (2004). This hinted at the potential of a segment-based approach for deciduous volume- and biomass modelling. The diverse structure of deciduous growth therefore lends itself to segment-based approaches, while small-radius plot-level deciduous volume and biomass modelling are problematic due to stand variability and the large size (crown width) of old-growth deciduous trees. It was concluded that segments encapsulated deciduous units better than a fixed plot-based approach.

Lower coniferous adjusted R^2 values found in this study were attributed to the diversity in coniferous segments, where a 2-class (deciduous-coniferous) modelling approach included segments with only marginally more coniferous than deciduous basal area. The associated increase in within-segment variability led to reduced adjusted R^2 values. However, there was no distinct difference between 2- and 3-class model metrics. Deciduous adjusted R^2 values ranged between 0.51 and 0.59 (2-class) and 0.52 and 0.62 (3-class), while coniferous values ranged between 0.46 and 0.66 (2-class) and 0.47 and 0.67 (3-class). Adjusted R^2 values for the mixed class in the 3-class scheme ranged between 0.43 and 0.74. It subsequently was concluded that a simpler, 2-class approach was preferable for the study area, while a 3-class scheme remains optional to the user, based on operational implications.

Model fit statistics generally deteriorated with increasing average segment size, although distinct differences among segment sizes were not evident. The exception was the 5.632 ha/segmentation result, with high adjusted R^2 values for coniferous ($R^2 \approx 0.66$), deciduous ($R^2 \approx 0.59$), and combined models ($R^2 \approx 0.54$). These relatively high values were attributed to better representation of BAF plot data at the larger segment size, while within-segment variability remained adequately small. The segment sizes between 0.091 ha/segment and 3.942 ha/segment, however, exhibited a general decreasing trend in adjusted R^2 values and an increasing trend in RMSE values. The lack of distinct differences among average segment sizes is an artefact of the hierarchical segmentation algorithm - within-segment variance was minimized at smaller segment size levels, with the hierarchical structure not further contributing in reducing within-segment variance. Results for the operational Appomattox stands, however, were distinctly lower than those found in the case of segmentation applications. Deciduous adjusted R^2 and RMSE values for volume modelling were 0.44 and 63.56 m^3/ha, while values for coniferous stands were 0.48 and 55.61 m^3/ha, respectively. Overall modelling results were 0.42 and 62.36 m^3/ha, which indicated that segmentation has distinct advantages over current defined stands in the study area. Relatively high adjusted R^2 values for 3-class coniferous volume ($R^2 \approx 0.73$) and biomass ($R^2 \approx 0.70$) were attributed to stand definition being based on homogenous, even-aged coniferous stands, but came at the cost of low adjusted R^2 values for deciduous stands.

Accuracies for the 2-class discriminant classification approach are shown in Figure 6. Overall accuracies ranged from 81.4% to 89.2% for the 2-class, deciduous-coniferous classification. It was concluded from the producer's and user's accuracies for the deciduous and coniferous classes that deciduous class assignment was more reliable than for coniferous objects. Kappa statistics for the 2-class classification ranged between 60.2% and 76.7%. Although overall and Kappa statistics peaked at 1.885 ha/segment, significant differences were only found between 1.885 ha/segment (89.2%) and 0.035 ha/segment (82.2%) and 0.964 ha/segment (81.4%) ($\alpha = 0.05$; $z = 1.96$). Overall accuracies for the 3-class, deciduous-coniferous-mixed classification ranged from 61.6% to 70.8%, while the Kappa statistics varied between 40.4% and 53.5%, with peak values again found at the 1.885 ha/segment segment-level. No significant differences were found in the case of the 3-class classification scheme. Significance testing indicated that there were minor to non-existing differences within the 2-class and 3-class schemes, but the T-test revealed a significance difference between the mean classification accuracies for the 2- and 3-class schemes at $\alpha = 0.05$ ($p < 0.001$). Producer's accuracies generally were highest for coniferous, followed by deciduous and mixed objects. User's accuracies typically decreased from deciduous to coniferous to mixed object classification.

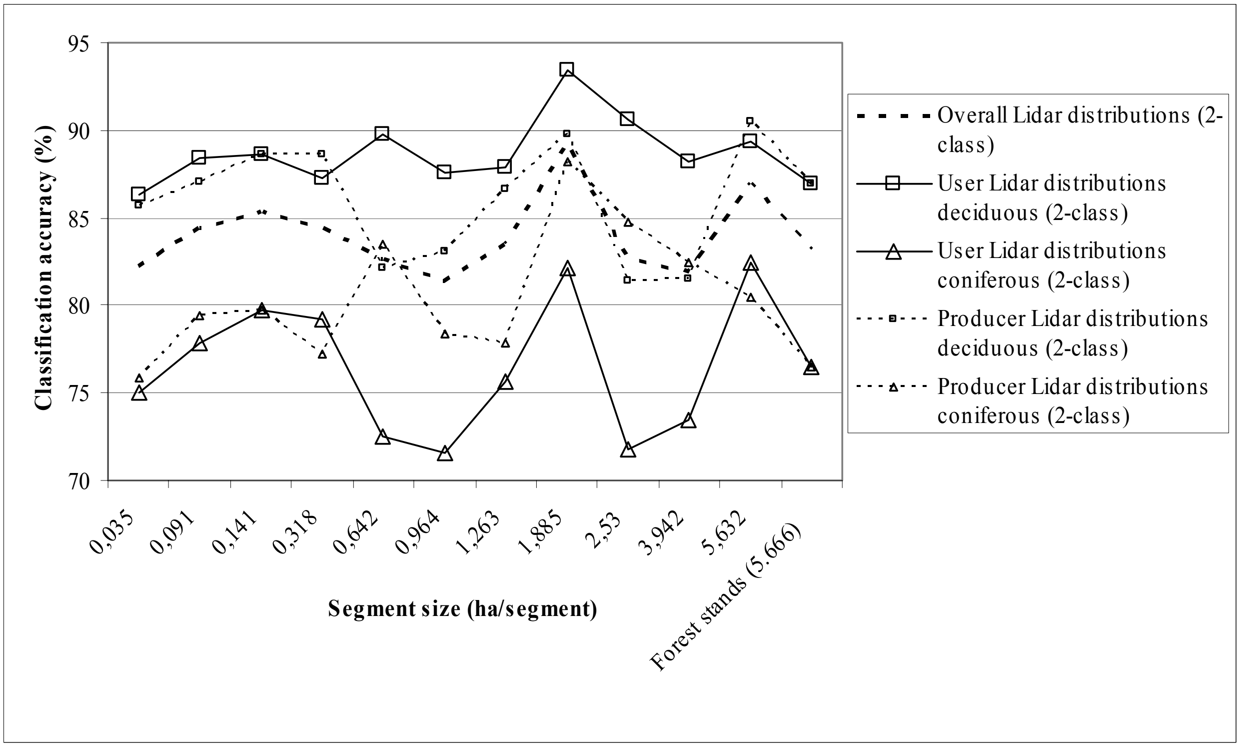

Figure 6. Overall, producer's, and user's classification accuracies for the 2-class classification based on lidar and CHM distributions

The following findings also are worth mentioning:

(i) Maximum classification accuracies generally were not statistical improvements over accuracy results for other segment sizes, indicating that average segment size did not influence classification for the study area. This result again was attributed to the hierarchical nature of the segmentation algorithm which merges smaller, homogenous segments to form larger segments at higher hierarchical levels.
(ii) The significance of the highest accuracies for the 2-class vs. 3-class scheme indicated that a deciduous-coniferous forest delineation was better suited to the Virginia Piedmont, as opposed to the inclusion of a mixed category as well. This was attributed to the forest types found in the study area, with most of the stands represented by one distinct taxonomic group and few completely mixed stands. Only 25 (11.4%) of the BAF plots were inherently part of a mixed class when a 75% basal area purity cut-off was used, further corroborating this conclusion.
(iii) The lack of a significant difference between segment-based classification and classification based on existing forest stands in the study area was ascribed to the definition of forest stands in an operational context. Forest stands are more often defined by their species make-up (coniferous-deciduous-mixed) than by their height structure (even-aged vs. all-aged). This effectively made the Appomattox stand map a thematic species map. However, classification accuracies were very encouraging if one considers that classification of segments was based on forest structure and not forest type definition.

Conclusions

Deciduous and coniferous volume and biomass modelling results based on object-oriented (segment) analysis were very promising, even though coniferous and combined adjusted R^2 values for volume and biomass were lower than those found in other published studies. Lower coniferous R^2 values were attributed in part to a smaller range of volume and biomass observed values, as well as to the inherent variability found in Virginia Piedmont forests. Adjusted R^2 values for deciduous segments were higher than those found for a comparable, plot-level study in the same area. This result indicated that a segment-level approach to deciduous volume and biomass modelling is a potential improvement over plot-based approaches, while the lack of modelling differences across varying segment sizes was attributed to the hierarchical nature of the segmentation algorithm. Segment-based modelling efforts were distinctly better than those found for existing, operational forest stands in the study area. This was attributed to the larger within-stand height variation in the case of existing stands when compared to the variation found within homogenous segments. RMSE values compared favourably with those found in other distributional modelling studies. Low RMSE values indicated that models could find applicability in an operational context, even when low R^2 values were considered.

Modelling and classification variables spanned the whole spectrum of possibilities, from general mean and range height values, to more abstract coefficient of variation and standard deviation-type variables. Regular and canopy cover percentiles also were well represented. The inclusion of intensity variables was interesting since few studies have included intensity values as part of forest biophysical modelling, even though these variables have proven to be useful for forest classification attempts. The wide range of variables indicated that sophisticated lidar scanners, capable of recording multiple returns and intensity associated with each lidar return, might well be necessary for effective modelling of variation in more complex forests.

Object-oriented classification results, as high as 89.2% (2-class scheme), were promising when one considers the type of input data and the variability in natural ecosystems. The absence of a decreasing classification accuracy trend at larger segment sizes again was attributed to the hierarchical nature of the segmentation algorithm. Stand-based classification also was not significantly different from segment-based approaches, which was attributed to the definition of operational forest stands on a per-species or type basis.

The increased classification accuracies for the 2-class forest type definition (deciduous-coniferous), as opposed to a 3-class (deciduous-coniferous-mixed) approach, was ascribed to high basal area percentages, in terms of deciduous or coniferous types, that had to be used for mixed class definition. This mixed class subsequently was closely associated with the deciduous group, resulting in reduced deciduous producer's accuracies. Higher producer's accuracies for the coniferous class (3-class scheme) indicated that the deciduous-mixed classes were main contributors to lower overall accuracies with increased between-group confusion.

Forest managers strive to obtain estimates of volume-by-type with high economical and statistical efficiency. The approach presented here would constitute a stand-alone forest inventory based on remote sensing inputs, but further research is needed to determine the associated precision and cost. The hierarchical nature of object-oriented approaches also is amenable to recombination of object-level results to any required scale. Lastly, the simplicity of the approach is attractive, since only per-object height/intensity values are potentially required. The synoptic coverage provided by remote sensing technologies could enable extension to net primary productivity modelling efforts, while local, sampling-based applications are not excluded.

Acknowledgements

Research was funded by NASA (grant # NG65-10548; NG613-03019), the McIntire-Stennis Research Program (grant # VA-136589), the Forestry Department and Graduate Student Assembly at Virginia Polytechnic Institute and State University, and the Potomac chapter of the American Society for Photogrammetry and Remote Sensing. The Virginia Department of Forestry, specifically Dr. John Scrivani, Todd Edgerton, Ralph Toddy, and Wayne Bowman (VDOF) contributed to field data collection. Dr. Sorin Popescu (Texas A&M University) provided invaluable assistance with statistical and lidar analyses. Amy Zhang from the Statistics department at Virginia Polytechnic Institute and State University served as statistical consult.

References

Avery, T.E. & Burkhart H.E. 1994. Forest Measurements. 4th Edition. McGraw-Hill, Boston, USA. 408 p.

Baatz, M. & Schäpe A. 2000. Multiresolution segmentation – an optimization approach for high quality multi-scale image segmentation. In: STROBL, J. *et al.* (Hrsg.): Angewandte Geographische Informationsverarbeitung XII. Beiträge zum AGIT-Symposium Salzburg, September 2000, Karlsruhe, Herbert Wichmann Verlag: 12–23.

Brandtberg, T., Warner T.A., Landenberger R.E. & McGraw J.B. 2003. Detection and analysis of individual leaf-off tree crowns in small footprint, high sampling density lidar data from the eastern deciduous forest in North America. *Remote Sensing of Environment* 85(2003):290-303.

Burrough, P.A. & McDonnel R.A. 1998. Principles of geographical information systems. Oxford University Press. Oxford, England. 333 p.

Clark III, A., Phillips D.R. & Frederick D.J. 1986. Weight, volume, and physical properties of major hardwood species in the Piedmont. USDA Forest Service, Southeastern Forest Experiment Station Research Paper SE-255, June 1986.

Congalton, R.G. & Green, K. 1999. Assessing the accuracy of remotely sensed data: Principles and practices. Lewis Publishers, New York, 137 p.

Cortijo, F.J. & De la Blanca N.P. 1999. The performance of regularized discriminant analysis versus non-parametric classifiers applied to high-dimensional image classification. *International Journal of Remote Sensing* 20(17):3345-3365.

Douglas, T.E., Evans D.L., Belli K.L. & Roberts S.D. 2003. Classification of pine and hardwood by the distribution and intensity of lidar returns. ISPRS “Three dimensional mapping workshop from InSAR and LIDAR”, June 17-19, 2003, Portland, Oregon, USA. 5 p.

Drake, J.B., Dubayah R.O., Clark D.B., Knox R.G., Blair J.B., Hofton M.A., Chazdon R.L., Weishampel J.F. & Prince S.D. 2002. Estimation of tropical forest structural characteristics using large-footprint lidar. *Remote Sensing of Environment* 79(2002):305-319

Draper, N.R. & Smith H. 1981. Applied regression analysis. 2nd Edition. John Wiley and Sons, Inc. New York, USA. 709 p.
eCognition User's Manual, 2003. Definiens Imaging (www.definiens.com).
Foody, G.M. 2004. Thematic map comparison: Evaluating the statistical significance of differences in classification accuracy. *Photogrammetric Engineering & Remote Sensing* 70(5):627-633.
Hodgson, M.E., Jensen J.R., Schmidt L., Schill S. & Davis B. 2003. An evaluation of LIDAR- and IFSAR-derived digital elevation models in leaf-on conditions with USGS Level 1 and Level 2 DEMs. *Remote Sensing of Environment* 84(2003):295–308.
Kayitakire, F., Farcy C. & Defourny P. 2002. Ikonos-2 imagery potential for forest stands mapping. ForestSAT Symposium, Heriot Watt University, Edinburgh, August 5-9, 2002. 11 p.
Kressler, F., Kim Y. & Steinnocher K. 2003. Object-oriented land cover classification of panchromatic KOMPSAT-1 and SPOT-5 data. In: Proceedings of IGARSS 2003 IEEE, July 2003, Toulouse. 7 pp.
Lefsky, M.A., Cohen W.B., Acker S.A., Parker G.G., Spies T.A. & Harding D. 1999. Lidar remote sensing of the canopy structure and biophysical properties of Douglas-fir and western hemlock forests. *Remote Sensing of Environment* 70:339-361.
Lefsky M.A., Cohen W.B., Parker G.G. & Harding D.J. 2002. Lidar remote sensing for ecosystem studies. *Bioscience* 52 (1): 19-30.
Maclean, G.A. & Krabil W.B. 1986. Gross-merchantable timber volume estimation using an airborne lidar system. *Canadian Journal of Remote Sensing* 12(1):7-18.
Magnussen, S. & Boudewyn P. 1998. Derivations of stand heights from airborne laser scanner data with canopy-based quantile estimators. *Canadian Journal of Forest Research* 28:1016-1031.
Makela H. & Pekkarinen A. 2001. Estimation of timber volume at the sample plot level by means of image segmentation and Landsat TM imagery. *Remote Sensing of Environment* 77:66-75.
Martin, M.E., Newman S.D., Aber J.D. & Congalton R.G. 1998. Determining forest species composition using high spectral resolution remote sensing data. *Remote Sensing of Environment* 65:249 – 254.
Means, J.E., Acker S.A., Harding D.J., Blair J.B., Lefsky M.A., Cohen W.B., Harmon M.E. & McKee A. 1999. Use of large-footprint scanning airborne lidar to estimate forest stand characteristics in the western Cascades of Oregon. *Remote Sensing of Environment* 67:298-308.
Means J.E., Acker S.A., Fitt B.J., Renslow M., Emerson L. & Hendrix C.J. 2000. Predicting forest stand characteristics with airborne scanning lidar. *Photogrammetric Engineering & Remote Sensing* 66(11):1367-1371.
Montgomery, D.C, Peck E.A. & Vining G.G. 2001. Introduction to linear regression analysis. 3rd Edition. John Wiley and Sons, Inc. New York, USA. 641 p.
Næsset, E. 2002. Predicting forest stand characteristics with airborne scanning laser using a practical two-stage procedure and field data. *Remote Sensing of Environment* 80(2002):88-99.
Nelson, R., Krabill W. & Tonelli J. 1988. Estimating forest biomass and volume using airborne laser data. *Remote Sensing of Environment* 24:247-267.
Nilsson, M. 1996. Estimation of tree heights and stand volume using an airborne lidar system. *Remote Sensing of Environment* 56:1-7.
Nugroho, M., Hoekman D.H. & De Kok R. 2002. Analysis of the forests spatial structure using SAR and Ikonos data. Presented at ForestSAT Symposium Heriot Watt University, Edinburgh, August 5-9, 2002. 10 p.
Pekkarinen A. 2002. Image segment-based spectral features in the estimation of timber volume. *Remote Sensing of Environment* 82:349-359.

Popescu, S.C., Wynne R.H. & Nelson R.F. 2002. Estimating plot-level tree heights with lidar: Local filtering with a canopy-height based variable window size. *Computers and Electronics in Agriculture* 37(2002):71-95.
Popescu, S.C., Wynne R.H. & Scrivani J.A. 2004. Fusion of small-footprint lidar and multispectral data to estimate plot-level volume and biomass in deciduous and pine forests in Virginia, U.S.A. *Forest Science* (In press)
Riaño, D., Meierc E., Allgöwerc B., Chuviecoa E. & Ustin S.L. 2003. Modelling airborne laser scanning data for the spatial generation of critical forest parameters in fire behavior modelling. *Remote Sensing of Environment* 86(2003):177–186.
Saucier, R.J. & Clark III A. 1985. Tables for estimating total tree and product weight and volume of major southern tree species and species Groups. Southwide Energy Committee, American Pulpwood Association, Inc.
Schroeder, P., Brown S., Mo J., Birdsey R. & Cieszewski C. 1997. Biomass estimation for temperate broadleaf forests of the United States using inventory data. *Forest Science* 43: 424 – 434.
Seielstad, C.A. & Queen L.P. 2003. Using airborne laser altimetry to determine fuel models for estimating fire behavior. *Journal of Forestry* 101(4):10-15.
Sharma, M. & Oderwald R.G. 2001. Dimensionally compatible volume and taper equations. *Canadian Journal of Forest Research* 31(5):797-803.
van Aardt, J.A.N. & Wynne R.H. 2001. Spectral separability among six southern tree species. *Photogrammetric Engineering & Remote Sensing* 67(12):1367-1375.